Limnol. Oceanogr., 53(3), 2008, 997–1013

Mass coral spawning: A natural large-scale nutrient addition experiment

Bradley D. Eyre[1]
Centre for Coastal Biogeochemistry, Southern Cross University, P.O. Box 157, Lismore, NSW 2480, Australia

Ronnie N. Glud[2]
Marine Biological Laboratory, University of Copenhagen, Helsingor, Denmark

Nicole Patten
Centre for Coastal Biogeochemistry, Southern Cross University, P.O. Box 157, Lismore, NSW 2480, Australia

Abstract

A mass coral spawning event on the Heron Island reef flat in 2005 provided a unique opportunity to examine the response of a coral reef ecosystem to a large episodic nutrient addition. A post-major spawning phytoplankton bloom resulted in only a small drawdown of dissolved inorganic phosphorus (DIP minimum = 0.37 μmol L^{-1}), compared with almost complete removal of dissolved inorganic nitrogen (DIN) (minimum NO_3^- = 0.01 μmol L^{-1}; NH_4^+ = 0.11 μmol L^{-1}), suggesting that pelagic primary production is potentially N limited on the timescale of this study. DIN, DIP, dissolved organic nitrogen (DON), and dissolved organic phosphorus were used in the production of biomass, and mass balance calculations highlighted the importance of organic forms of N and P for benthic and pelagic production in tropical coral reef environments characterized by low inorganic N and P. The input of N and P via the deposition of coral spawn and associated phytodetritus resulted in large changes to N cycling in the sediments, but only small changes to P cycling, because of the buffering capacity provided by the large pool of bioavailable P. It is most likely that this large pool of bioavailable P in the sediments drives potential N limitation of benthic coral reef communities. For example, there was sufficient bioavailable P stored in the top 10 cm of the sediment column to sustain the prespawning rates of benthic production for over 200 d. Most of the change in benthic N cycling occurred via DON and N_2 pathways, driven by changes in the quantity and quality of organic matter deposited and decomposed post-major spawning. The heterotrophic and autotrophic microbial communities within the coral reef sands were able to rapidly (6 to 7 d) process the large episodic load of N and P provided by coral mass spawning.

Mass coral spawning or smaller-scale multispecific coral spawning events have been observed on coral reefs around the world (Harrison et al. 1984; Hayashibara et al. 1993; Hagman et al. 1998). In the central Great Barrier Reef (GBR) (Australia) mass spawning typically occurs on the third to sixth night after a full moon in October to December (Harrison and Wallace 1990). Synchronous multispecies coral spawning releases a large volume of eggs (1×10^6 m^{-2}) and sperm to the water column over a short period of time (Harrison and Wallace 1990). Large slicks of coral spawn products can form on the water surface and beaches of coral reef lagoons. Some of these eggs and sperm, which have a high lipid content (Arai et al. 1993), can be trapped within the coral reef lagoon (Wolanski et al. 1989; Simpson et al. 1993), resulting in a large episodic input of labile carbon (and associated nitrogen and phosphorus) to the coral reef ecosystem. For example, an estimated 310,000 kg of C and 18,000 kg of N were released from coral eggs alone (sperm not included) during a coral spawning event at the Heron Island reef in 2001 (Wild et al. 2004). As such, a coral spawning event represents a unique opportunity to examine the response of a coral reef ecosystem to a large episodic nutrient addition.

Despite the potential for this large input of labile carbon to modify coral reef biogeochemistry and pelagic and benthic food webs, little work on the effects of coral spawning on the energy and nutrient cycles of coral reef ecosystems has been undertaken. Wild et al. (2004) measured a 2.5-fold increase in sediment oxygen demand after a spawning event on Heron Island in the GBR, reflecting an input of labile carbon and subsequent decomposition in permeable coral reef lagoon sediments. Similarly, Simpson et al. (1993) recorded a dramatic decrease in water column dissolved oxygen on Ningaloo Reef after mass coral spawning, resulting in mass mortality of fish and other reef animals due to the respiratory demand of the coral spawn. Glud et al. (2008) found that nutrients released after coral spawning not only stimulated the heterotrophic communities but also the autotrophic communities with 4.0- and 2.5-factor increases in pelagic

[1] Corresponding author (bradley.eyre@scu.edu.au).
[2] Present address: Scottish Association for Marine Science (SAMS), Marine Laboratory Dunbeg, Oban, Argyll PA37 1QA, Scotland, United Kingdom.

Acknowledgments

We thank Iain Alexander and Anni Glud for assistance with the laboratory work and data compilation and analysis and Tage Dalsgaard for running the anammox samples.

This work was supported by an ARC Discovery Grant (DP0342956) awarded to B.D.E., and an SCU Visiting Researcher Fellowship and NSF (Denmark) grants awarded to R.N.G. and was carried out under permit G06/18413.1.

and benthic production, respectively. Several studies have also found a direct transfer of coral spawning products to higher trophic levels via grazing by ophiuroids, zooplankton, and reef fish (Westneat and Resing 1988; Baird et al. 2001; Pratchett et al. 2001).

The tropical waters surrounding coral reefs are mostly devoid of macronutrients, giving rise to the paradigm that primary production on coral reefs is typically nutrient limited. Numerous studies have found a N-limited response in benthic communities (Dizon and Yap 1999; Heil et al. 2004), and water column N : P ratios are typically <16 (Furnas et al. 1990; Charpy 2001), suggesting short-term N limitation of coral reef ecosystems. In addition, biogeochemical process in coral reef sediments such as denitrification have also been shown to increase after N additions (Koop et al. 2001). Some of the short-term N limitation of benthic communities (e.g., benthic microalgae) may be driven by the large sediment pool of P (Entsch et al. 1983; Suzumura et al. 2002). In the longer term, however, coral reef ecosystems may ultimately be P limited because N can be replenished via N fixation, which has been shown to increase after P additions (Koop et al. 2001).

As such, we expect to see differences in the way N and P will be cycled via both the stimulated benthic and pelagic heterotrophic and autotrophic communities after the large nutrient addition associated with coral spawning. This natural whole ecosystem-scale nutrient addition experiment should provide unique insight into N versus P limitation of coral reef ecosystems, and how the system processes a large pulse of nutrients that is not obtainable using smaller-scale experimental work.

To assess the effects of coral spawning on N and P cycling in a coral reef ecosystem we measured diurnal changes in water column N and P, light and dark benthic N and P fluxes, and denitrification immediately before and daily for 7 d after coral spawning on a Heron Island reef flat, Australia. Measurements of anammox, N fixation, N deposition rates, and sediment solid-phase N and P concentrations were also performed before and after coral spawning.

Materials and methods

Study site—All sampling was undertaken at one site in the middle of a Heron Island reef flat between 18 and 28 November 2005. Heron Island is at the southern end of the GBR about 70 km off the coast of Gladstone, Australia. The reef flat is a mosaic of different coral species and coarse carbonate sands. Overall 48% of the reef flat at Heron Island consists of sand. The findings from this study would be applicable to other parts of the Heron Island reef system because 85% of the lagoon and 85% of the lagoon edge also contain sand (Roelfsema et al. 2002). During the study period the water depth at the study site varied between about 300 mm and 1,800 mm, with many of the corals exposed to air at low tide. Sediment porosity ranged from 0.57 ± 0.02 (vol : vol) at the surface to 0.52 ± 0.02 (vol : vol) at 10 cm depth and sediment permeability ranged from $6.0 \pm 0.7 \times 10^{-11}$ m^{-2} (0 to 0.5 cm depth) to $1.6 \pm 0.6 \times 10^{-11}$ m^{-2} (5 to 10 cm depth) (Glud et al. 2008).

Water column sampling—Water column sampling was undertaken over 10 consecutive days from 18 to 27 November 2005. On each day samples were collected at 05:00 h (dawn), 13:00 h (midday), and 18:00 h (dusk) from the middle of the well-mixed water column in two 1-liter acid-washed and sample-rinsed polyethylene containers and transported to the laboratory within 10 min. In the laboratory 20 mL of sample were immediately filtered through a 0.45-μm cellulose acetate membrane filter (Sartorius) into two acid-washed and sample-rinsed 10-mL polyethylene vials. An unfiltered sample was collected in an acid-washed and sample-rinsed 10-mL polyethylene vial for total nutrient analysis. All nutrient samples were immediately frozen at -20°C. Details of the nutrient analysis are given in Eyre (2000). The day after major coral spawning, a sample of the spawn slick was collected from the water surface near the study site in two 70-mL acid-washed and sample-rinsed polyethylene containers and immediately frozen at -20°C.

Benthic incubations—Benthic incubations were undertaken over 9 consecutive days from 20 to 28 November 2005. At 18:00 h on each day duplicate round benthic chambers with an internal diameter (i.d.) of 190 mm and a height of 330 mm (Huettel and Gust 1992) were inserted into the carbonate sands between outcrops of coral to retain a water column height of 190 to 240 mm and left uncapped for 3 h to equilibrate. The chambers were stirred at 40 revolutions per minute (rpm) to induce advective flow through the permeable carbonate sands. On the eighth day one of the 40-rpm chambers was stirred at 80 rpm, while another was stirred in diffusive mode (i.e., alternating stirring direction with no steady partial pressure gradient; Cook et al. 2006), giving a gradient of advective flow (diffusive, 40 rpm, 80 rpm). On the basis of the initial sediment permeability, temperature, and salinity the stirring rates of 40 and 80 rpm would have induced sediment percolation rates of approximately 43 and 213 L m^{-2} d^{-1} respectively (Glud et al. 2008). Each of the nine benthic incubations was undertaken over a full diel cycle. The first samples from the chambers were collected at 21:00 h; the chambers were then capped, and subsequent samples were collected at 02:00 h, 05:00 h (dawn), 10:00 h, and 17:00 h (dusk). N_2 : Ar samples were only collected at nighttime as the formation of bubbles during daytime confounded any gas samples. At 18:00 h the chambers were then moved within a 500 m^2 area and again left uncapped for 3 h to equilibrate before restarting the sampling cycle. Oxygen concentrations within the closed chambers closely followed the water column concentrations (Glud et al. 2008). On each sampling occasion two 50-mL presoaked (in site water) plastic syringes of water were collected from each chamber, and as a sample was withdrawn an equal amount was replaced from the bottom water. Within 10 min of sampling, 20 mL of sample were transferred to a polyethylene vial for dissolved oxygen measurements, and 20 mL of sample were immediately filtered through a 0.45-μm cellulose acetate membrane filter (Sartorius) into two 10-mL acid- and sample-rinsed polyethylene vials. To minimize the introduction of bubbles, N_2 : Ar samples were

collected in triplicate 7-mL gas-tight glass vials with glass stoppers by adding a piece of gas-tight tubing to the syringe and filling from the bottom of the vial until it overflowed. All nutrient samples were immediately frozen at −20°C. N_2 : Ar samples were poisoned with 20 μL of 5% $HgCl_2$ and stored submerged at ambient temperature. Details of the nutrient and N_2 : Ar analysis are given in Eyre et al. (2002) and Eyre and Ferguson (2005). Dissolved oxygen measurements were undertaken using a HACK LDO HQ-10 and checked against Winkler titrations (*see* Glud et al. 2008). The oxygen and dissolved inorganic carbon data are presented elsewhere (Glud et al. 2008).

Benthic flux calculations—Fluxes across the sediment–water interface were calculated by linear regression of the concentration data, corrected for the addition of replacement water, as a function of incubation time, core water volume, and surface area. Dark flux rates were calculated using concentration data from 21:00 h to 05:00 h and light flux rates were calculated using concentration data from 05:00 h to 17:00 h.

$$\text{Net flux rates} = ([\text{dark rates} \times \text{hours of darkness}] + [\text{light rates} \times \text{hours of daylight}])/21\ \text{h}$$

Nitrogen fixation and anammox—Triplicate 50-mm cores of sediment (150-mm depth) were collected on 20 (pre-major spawning) and 26 (5 d post-major spawning) November 2005. The top 30 mm and the 30- to 120-mm depth of the three cores were homogenized to provide composite samples of two depths. Approximately 4.00 g (±10 mg) of sediment were added to 12 exetainers from each depth for N fixation measurements and 16 exetainers for each depth for anammox measurements. The N-fixation exetainers were filled with 10% acetylene-saturated filtered site water and the anammox exetainers were filled with filtered site water and both sets of exetainers were then bubbled with N_2 for 5 min to remove oxygen. Four anammox series were established by adding 50 μL of 10 mmol L^{-1} $^{15}NH_4$, 50 μL of 10 mmol L^{-1} $^{15}NH_4$ + 50 μL of 10 mmol L^{-1} $^{15}NO_3$, 50 μL of 10 mmol L^{-1} $^{15}NO_3$ + 50 μL of 10 mmol L^{-1} NH_4, and 50 μL of 10 mmol L^{-1} $^{15}NO_3$ each to four of the anammox exetainers. All exetainers were incubated in the dark at in situ temperature and 200 μL of 50% $ZnCl_2$ was added to triplicate N fixation and one of each anammox series at approximately 6.5, 11.5, 16, and 24 h after the incubations were started to establish a time series (Rysgaard et al. 2004). $^{14}N^{15}N$ and $^{15}N^{15}N$ enrichment was analyzed on a gas chromatograph coupled to a triple-collector isotopic ratio mass spectrometer (Rysgaard-Petersen and Rysgaard 1995) and relative anammox rates were calculated as described by Thamdrup and Dalsgaard (2002).

Analysis of ethylene concentrations was undertaken by withdrawing a 100-μL gas sample from the 5-mL gas headspace of the exetainer and analyzed using a Hewlett Packard 6890 gas chromatograph with a GS "Gaspro" column (30 m × 0.53 i.d.) and flame ionization detector. Ethylene concentrations were corrected using standards produced from serial dilution of analytical-grade ethylene. Ethylene concentration change as a function of time (linear regression) was then used to calculate the rates of ethylene production per gram of sediment. A conversion ratio of 4 : 1 was used to convert ethylene concentrations to N_2 (Capone 1993).

Solid-phase sediment—Triplicate 50-mm cores of sediment (150-mm depth) were collected daily from 23 to 29 November 2005 at the same location as the benthic incubations. The cores were subsampled at three depth intervals (0–1 cm, 4–5 cm, 6–7 cm) with the sediment placed into a 70-mL acid-washed and sample-rinsed polyethylene container and immediately frozen at −20°C. Inorganic carbon was removed by HCl fuming and organic carbon and nitrogen were analyzed by high-temperature combustion on Thermo Flash EA 1112. The bioavailable fraction of P (Colwell-P) was extracted by taking a 0.3-g sample of sediment or spawning material and mixing it with 30 mL of 0.5 mol L^{-1} $NaHCO_3$ adjusted to pH 8.5 with NaOH for 16 h at 25°C, then centrifuging and removing the supernatant (Birch et al. 1999). All P analyses of extracts were carried out colorimetrically after 1 : 10 dilutions. Standards were made in the same matrix as the extractant. Total phosphorus was extracted by digesting a 0.4-g sample of dried (60°C) sediment or spawning material in 2.5 mL of concentrated nitric acid and 7.5 mL of concentrated HCl for 1 h at 120°C. The volume was then made up to 25 mL with Milli-Q water and analyzed by inductively coupled plasma–optical emission spectrometry to determine the concentration of P.

Results

Coral spawning and associated observations—Minor coral spawning occurred on the night of 20 November with approximately 30% of the *Montipora digitata* releasing eggs. Major coral spawning occurred on the following night (21 November) with approximately three-quarters of observed *Acropora millepora* releasing eggs. The following day (22 November) there was a slight smell of decomposing spawning material (eggs, sperm) but no visible slicks on the water surface. Many massive corals (e.g., by *Platygyra daedalea*) spawned on the night of 22 November. By day 2 post-major spawning (23 November), large quantities of spawning material was visible on the water surface (Glud et al. 2008) and suspended in the water column, which dramatically reduced visibility. By day 3 post-major spawning (24 November) most of the visible slick of spawning material on the water surface was gone, but the water column was still turbid with decomposing spawning material. The spawning material induced benthic and pelagic microalgal blooms (Glud et al. 2008).

Water column—The coral spawning material had a C content of 50.8 ± 4.2 mmol g^{-1}, a N content of 2.5 ± 0.4 mmol g^{-1}, and a P content of 0.16 ± <0.01 mmol g^{-1}, giving a molar C : N : P ratio of approximately 316 : 16 : 1. Total nitrogen (TN) concentrations in the water column ranged from 6.00 to 18.45 μmol L^{-1} over the study period

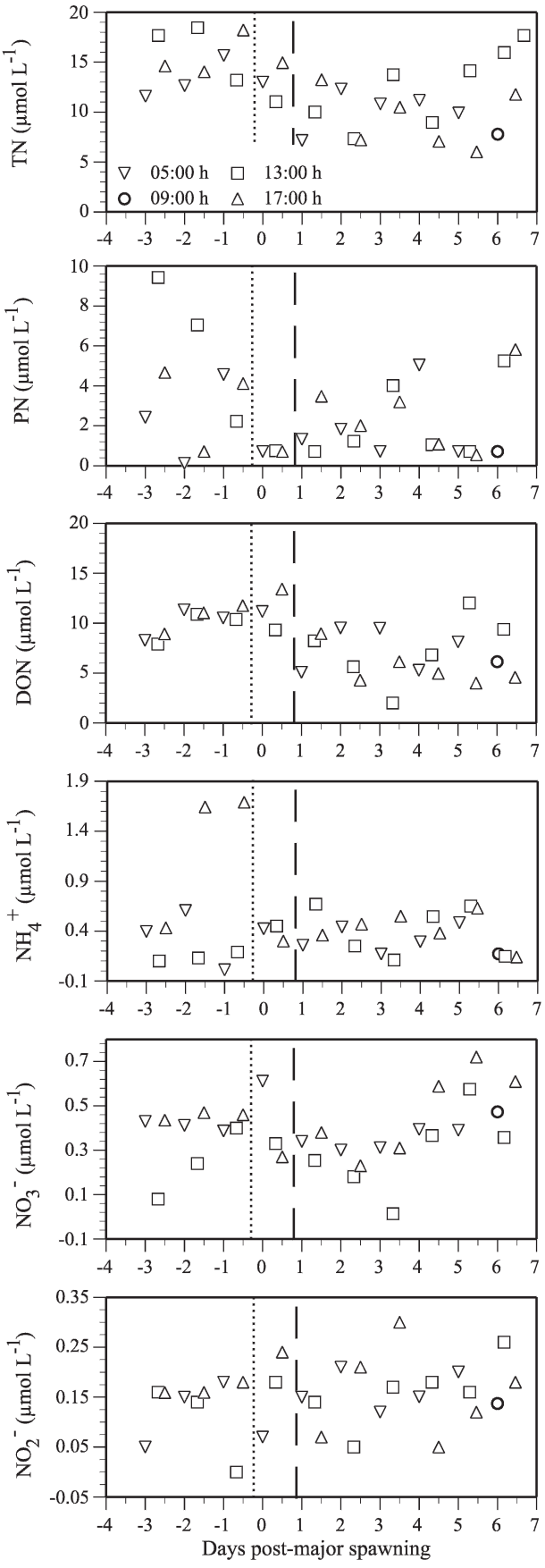

(Fig. 1). Most of the TN consisted of dissolved organic nitrogen (DON) (average 71%) and particulate nitrogen (PN) (average 20%). Ammonium (NH_4^+), nitrate (NO_3^-), and nitrite (NO_2^-) concentrations were mostly below 0.60, 0.40, and 0.20 μmol L^{-1} respectively, and combined (dissolved inorganic nitrogen, DIN) only made up a small proportion of the TN (average 9%). Dusk and dawn TN concentrations increased from the start of the study period through the prespawning period to a maximum immediately before minor spawning (Fig. 1). DIN and DON concentrations generally decreased postspawning, with the midday samples approaching the detection limit, and then increased toward the end of the study period. PN concentrations were highly variable and showed no distinct pattern.

Total phosphorus (TP) concentrations ranged from 1.20 to 1.75 μmol L^{-1} and mostly consisted of dissolved organic phosphorus (DOP) (average 59%) (Fig. 2). Dissolved inorganic phosphorus (DIP) concentrations ranged from 0.35 to 0.49 μmol L^{-1} and on average made up 31% of the TP (Fig. 1). Particulate phosphorus (PP) was only a small fraction of the TP (average 10%). TP and PP concentrations remained fairly constant over the study period, except for midday increases 2 to 6 d post-major spawning. In contrast, DIP and DOP concentrations were quite variable, but showed much smaller changes than DIN and DON and never approached the detection limit. DIP concentrations generally increased from the start of the study period through the prespawning period to a maximum post-minor spawning and then decreased immediately post-major spawning before increasing slightly toward the end of the study period. DOP concentrations showed the opposite trend, decreasing from the start of the study through the prespawning period and then increased post-minor spawning and remained fairly constant to the end of the study period. The increase in DIP post-minor spawning was less than the increase in DIN and hence DIN : DIP ratios also increased (Fig. 2). Similarly, the decrease in DIN 3 d post-major spawning was greater than the decrease in DIP and hence the DIN : DIP ratio dropped below 1 at midday.

Benthic fluxes (40 rpm)—With the exception of dark NH_4^+ fluxes switching from a prespawn uptake to an immediate (1 d) post-major spawning efflux (Fig. 3), the changes in NO_3^- and NH_4^+ fluxes were small and mostly linked to changes in N_2. DON fluxes were up to more than an order of magnitude greater than the DIN fluxes ($NH_4^+ + NO_3^-$), and as such, made up on average 39% of the total net benthic dissolved nitrogen flux (Fig. 3). They also showed significant ($p < 0.5$) changes over the study period. With the exception of the immediate (1 d) post-major spawning efflux of 144 μmol m^{-2} h^{-1}, dark DON fluxes generally progressed from a large prespawning uptake of -306 μmol m^{-2} h^{-1} to an efflux of 118 μmol m^{-2} h^{-1} over the study period. The light DON fluxes generally

←

Fig. 1. Water column nitrogen concentrations over the study period. Dotted line, minor spawning; dashed line, major spawning.

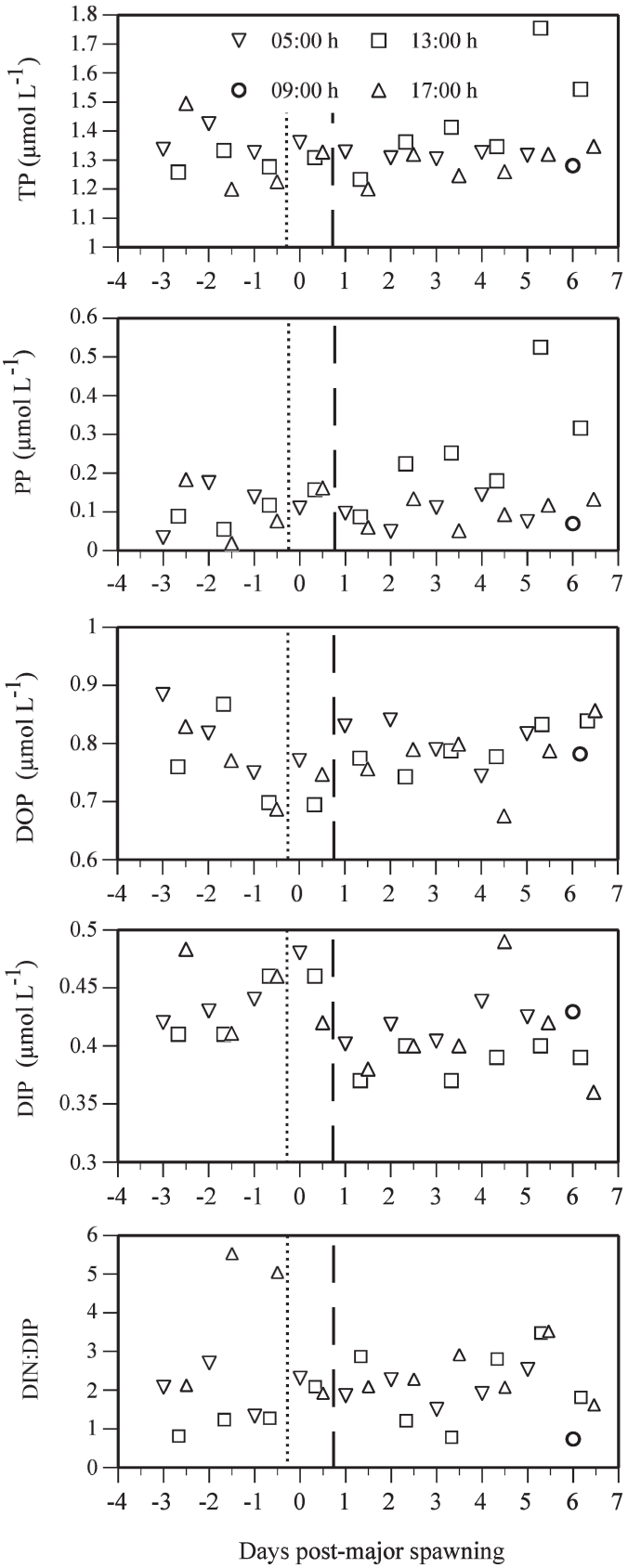

Fig. 2. Water column phosphorus concentrations over the study period. Dotted line, minor spawning; dashed line, major spawning.

progressed from a prespawning efflux of 21 μmol m^{-2} h^{-1} to an uptake of -297 μmol m^{-2} h^{-1} over the study period. Net DON uptakes decreased immediately post-major spawning, and remained lower for 5 d before returning to a similar uptake to prespawning by the end of the study period.

Dark N_2 fluxes were generally the largest of the N fluxes, making up on average 54% of the total net benthic dissolved N flux (on the basis of dark N_2 fluxes only) (Fig. 3). They also showed a significant ($p < 0.05$) change over the study period. Dark N_2 fluxes changed little from pre- to immediately (1 d) post-major spawning, but then increased rapidly, peaking 4 d post-major spawning at 240 μmol m^{-2} h^{-1}. The increase in N_2 efflux on day 4 post-major spawning corresponds to an increase in the dark efflux of NO_3^-, suggesting an increase in coupled nitrification–denitrification. The large N_2 efflux on day 5 post-major spawning corresponded to an increase in the uptake of both dark NO_3^- and NH_4^+, suggesting that both coupled nitrification–denitrification and denitrification of water column NO_3^- was occurring. By day 6 post-major spawning N_2 effluxes had decreased to the smallest rate of the study (18 μmol m^{-2} h^{-1}). There was no dark N_2 flux data for the last day of the study.

Except for dark DIP and the light DOP fluxes, the P fluxes showed no distinct changes over the study period (Fig. 3). Dark DIP uptakes decreased immediately post-minor spawning and remained lower for 5 d before increasing to a rate similar to the prespawning rate at the end of the study period. Light DOP fluxes switched from an almost zero (-0.06 μmol m^{-2} h^{-1}) prespawning flux to an uptake of -2.34 μmol m^{-2} h^{-1} immediately (1 d) post-major spawning. By day 2 post-major spawning light DOP fluxes had switched to an efflux, which increased to 1.97 μmol m^{-2} h^{-1} by day 3 post-major spawning. Light DOP fluxes then switched back to an uptake of -0.41 μmol m^{-2} h^{-1} by day 4 post-major spawning and decreased to a rate similar to the prespawning rate (-0.15 μmol m^{-2} h^{-1}) at the end of the study period. Overall the changes in the P fluxes were much smaller than the changes in the DON and N_2 fluxes.

Stirring gradient effects on benthic fluxes—Dark NO_3^- fluxes showed an increasing uptake with increasing advective flow (Fig. 4). In contrast, light fluxes showed a decreasing uptake with increasing advective flow and net fluxes showed no change (Fig. 3). Dark NH_4^+ fluxes switched from an efflux to an uptake as the pore-water flushing increased, although not proportionally to the change in advective flow rate. These switches from an efflux to an uptake corresponded to an increase in benthic O_2 consumption with increasing advective flow (Glud et al. 2008). DIP fluxes showed no consistent change with changing advective flow rate. In contrast, light and net NH_4^+ fluxes switched from an uptake to an efflux with a proportional increase with the increase in advective flow rate. This switch from an uptake to an efflux and proportional increase with advective flow also corresponds to an increase in benthic production with increasing advective flow (Glud et al. 2008). DON and DOP fluxes

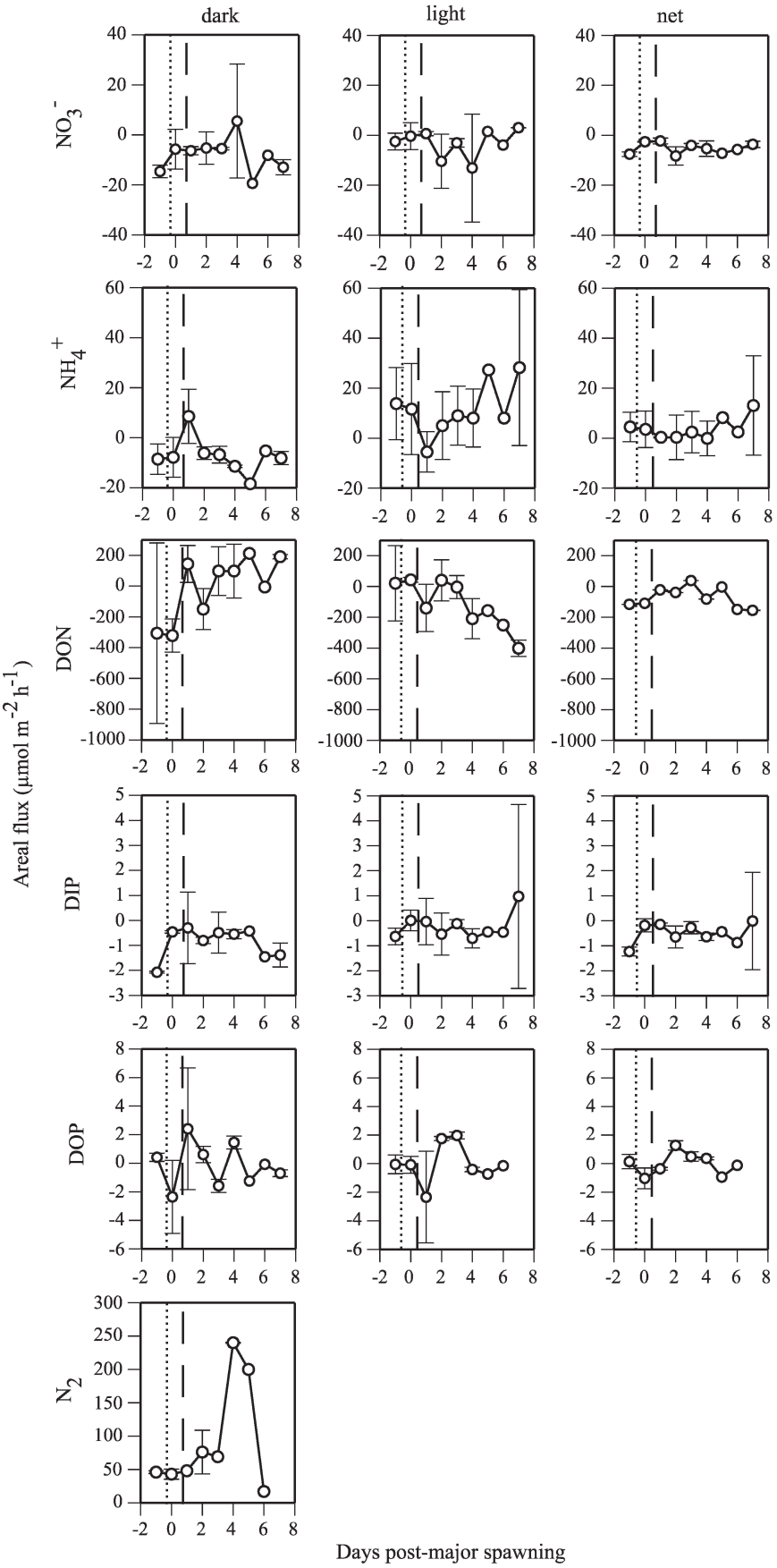
dark
light
net
NO_3^-
NH_4^+
DON
DIP
DOP
N_2
Areal flux (μmol m^{-2} h^{-1})
Days post-major spawning

mostly showed a proportional change with changes in advective flow, but the direction of change varied between incubations and light and dark. The proportional decrease in net DON and DOP uptake with increasing advective flow also corresponded to an increase in benthic production with increasing advective flow (Glud et al. 2008). Dark N_2 fluxes consistently changed from a diffusive uptake to an increasing efflux as the advective flow increased.

Sediment nitrogen, phosphorus, anammox, nitrogen fixation—Sediment N concentrations averaged 28.6 μmol g^{-1} and showed no significant change over depth or time ($p = 0.05$). No anammox was detected during this study. N-fixation rates for the top 30 mm of sediment ranged from 0.29 nmol g^{-1} h^{-1} N_2 (5.0 μmol m^{-2} h^{-1} N_2) prespawning to 0.18 nmol g^{-1} h^{-1} N_2 (3.0 μmol m^{-2} h^{-1} N_2) postspawning, and from 0.45 nmol g^{-1} h^{-1} N_2 (18.7 μmol m^{-2} h^{-1} N_2) prespawning to 0.18 nmol g^{-1} h^{-1} N_2 (7.5 μmol m^{-2} h^{-1} N_2) postspawning for the 30-mm to 120-mm depth.

Total sediment P showed no significant ($p = 0.05$) change with depth, or over the study period, and averaged about 7.9 μmol g^{-1} P (Fig. 5), which is similar to the concentrations reported for other coral reef sediments (e.g., Entsch et al. 1983; Erftemeijer and Middelburg 1993; Suzumura et al. 2002) and nearshore sediments in the GBR (Eyre 1993). In contrast, bioavailable sediment P concentrations in the 0- to 1-cm and 4- to 5-cm depths showed a significant ($p = 0.05$) decrease from 1 d post-major spawning to the end of the study (Fig. 5). We have no prespawning sediment P data, but the decreasing concentrations post-major spawning suggest that the deposition of spawning material resulted in an increase in bioavailable P concentrations in the top of the sediment profile, which subsequently decreased over the study period. At the 6- to 7-cm depth bioavailable P reached a maximum concentration on day 2 post-major spawning, suggesting that it took a day for the spawning material to percolate to the lower layers. The input of bioavailable P to the sediments is best illustrated by its percentage contribution to total P, which decreased from 15% to 10% at 0- to 1-cm depths and from 18% to 10% at 4- to 5-cm depths over the study period. Previous estimates of the percentage contribution of bioavailable P to total P in coral reef sediments have ranged from 1% to 32% depending on the strength of the extractant used to extract P (e.g., Entsch et al. 1983; Erftemeijer and Middelburg 1993; Suzumura et al. 2002).

Discussion

Water column—An increase in nutrient availability after mass spawning induced a fourfold increase in pelagic production 1 d post-major spawning (Glud et al. 2008), but this was not clearly reflected in the nutrient concentration data, which only showed small changes. Although the concentration changes were only small, they occurred against a background of large advective tidal flow across the reef, suggesting that the processes driving these changes were significant. Similar episodic increases in phytoplankton production and biomass due to nutrient enrichment after a cyclone has been seen in barrier and fringing reefs in French Polynesia (Delesalle et al. 1993). Small prokaryotes that typically dominate phytoplankton biomass in the GBR lagoon are able to begin bloom formation <1 d after episodic increases in DIN of as little as 0.1 μmol L^{-1} (Furnas et al. 2005).

The phytoplankton bloom resulted in the almost complete removal of NO_3^- (0.01 μmol L^{-1}) and NH_4^+ (0.11 μmol L^{-1}) 3 d post-major spawning, but only a small drawdown of DIP, suggesting that N is potentially limiting to pelagic primary production on the timescale of this study (days). Pelagic productivity rates had already decreased by this stage (Glud et al. 2008), suggesting that phytoplankton production had become nutrient limited. From 1 to 5 d post-major spawning both midday DIN and DON were negatively correlated with PN ($r^2 = 0.61$ and $r^2 = 0.69$ respectively; not significant at $p = 0.05$), and both DIP ($r^2 = 0.50$; $p < 0.01$; all data) and DOP ($r^2 = 0.51$; $p < 0.05$; 13:00 h data only) were significantly correlated with water column oxygen concentrations, suggesting that both forms of N and P were utilized in the production of biomass. This highlights the importance of DON and DOP in tropical coral reef environments that are low in inorganic N and P. Pelagic productivity had returned to prespawning rates by day 6 post-major spawning, which is reflected in an increase in DIN and DON as the bloom collapsed and nutrients were recycled to the water column (Fig. 1). This tropical coral reef lagoon boom–bust sequence due to episodic inputs of nutrients from coral spawning is similar to the boom–bust sequence in tropical estuaries associated with episodic inputs of nutrients from floods (Eyre and Ferguson 2006).

Effect of coral spawning on benthic fluxes—Coral spawning material is rapidly incorporated into the sediments of coral reef lagoons either directly via sedimentation (advective-driven percolation) (Wild et al. 2004; Glud et al. 2008) or indirectly via the deposition of phytodetritus from phytoplankton and benthic microalgae (BMA) stimulated by nutrient release associated with spawning (Glud et al. 2008) and deposition of fecal pellets from fish and zooplankton that feed on spawning material (Westneat and Resing 1988; Baird et al. 2001; Pratchett et al. 2001). This input of labile carbon after the spawning event we studied resulted in a twofold increase in benthic O_2 consumption and the release of N associated with the decomposition of spawning material and phytodetritus in the sediments also stimulated a 2.5-fold increase in net benthic primary production (Glud et al. 2008). These changes in benthic respiration and production associated

←

Fig. 3. Benthic nitrogen and phosphorus fluxes at 40 rpm over the study period (mean ± SD; $n = 2$). Dotted line, minor spawning; dashed line, major spawning.

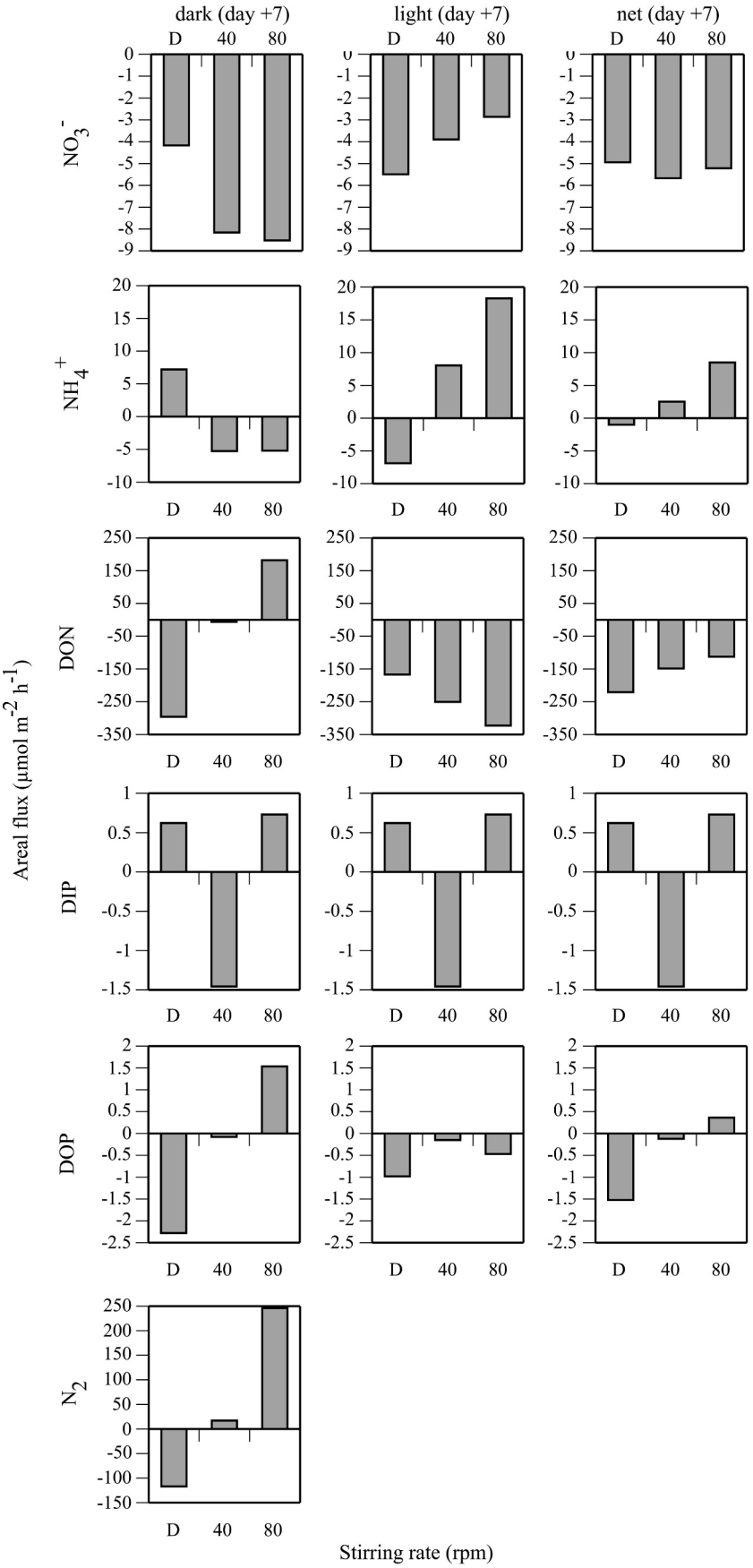
dark (day +7)
light (day +7)
net (day +7)
D 40 80
NO3 -
NH4 +
DON
DIP
DOP
N2
Areal flux (µmol m-2 h-1)
Stirring rate (rpm)

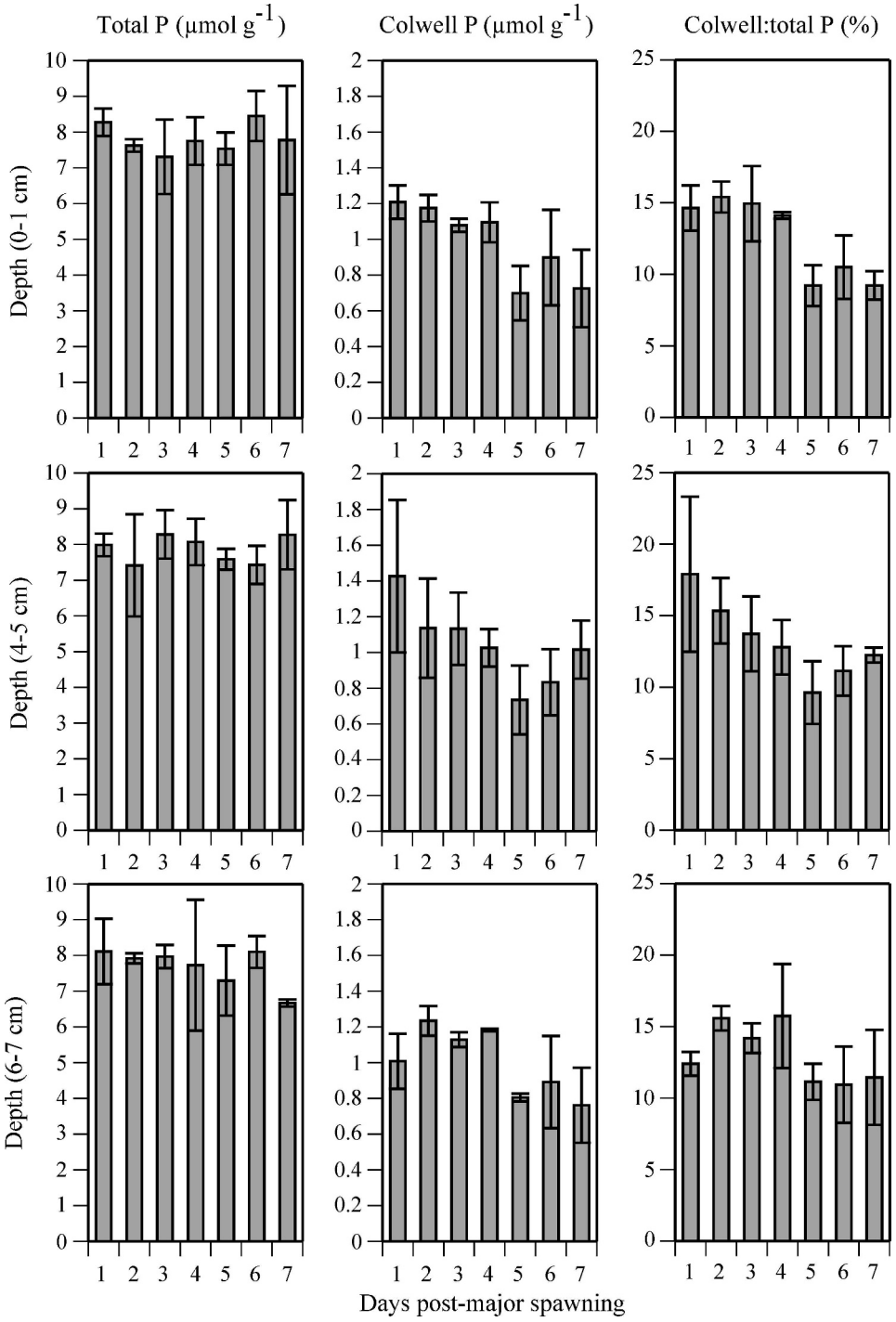

Fig. 5. Sediment total and bioavailable phosphorus concentrations. Also shown is the percentage contribution of bioavailable phosphorus to total phosphorus.

←

Fig. 4. Benthic nitrogen and phosphorus fluxes over a stirring gradient day 7 post-major spawning. D = diffusive.

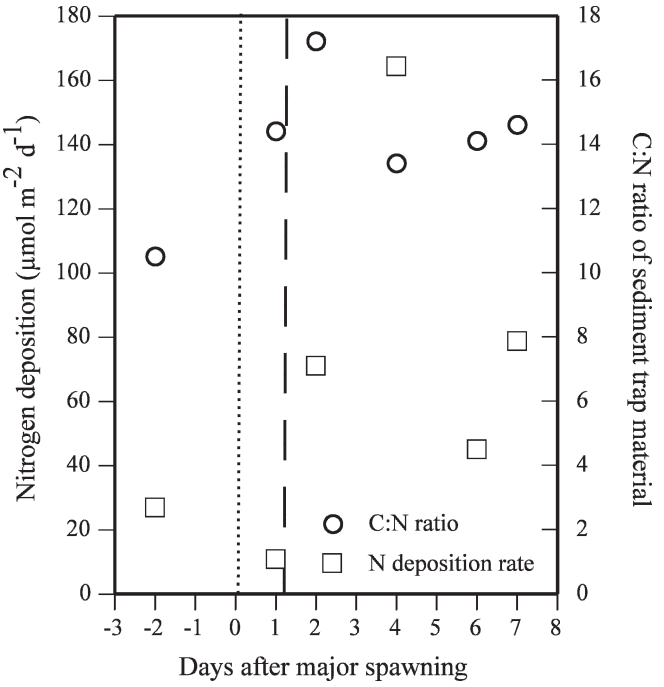

Fig. 6. Sediment trap data modified from Wild et al. (2007). The sample site was located approximately the same distance from the shore and 100 m to the east of our sample site. Dotted line, minor spawning; dashed line, major spawning.

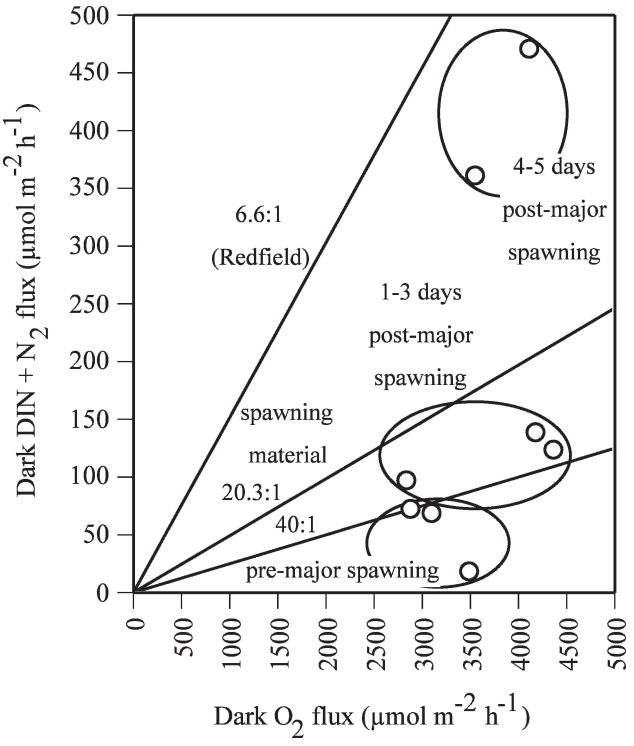

Fig. 7. Dark O_2 flux versus dark DIN + N_2 flux.

with coral spawning significantly modified the cycling of N in the sediments, but only resulted in small changes to the cycling of P in the sediments. Although the rates and pathways of benthic N and P cycling processes were modified after coral spawning, most had return to prespawning conditions by the end of the study period, illustrating the rapid processing of the nutrient pulse by the microbial communities.

Benthic heterotrophic metabolism and nutrient cycling—Benthic metabolism and N cycling was primarily driven by the quantity and quality of organic matter (OM) deposition over the study period. The sequence of pelagic events (source of OM), the dark O_2 and N benthic flux stoichiometry, and the deposition rates and C : N ratios of sediment trap material (Wild et al. 2008) together suggest three distinct OM depositional events: (1) prespawning and 6 d or more post-major spawning (subsequently referred to as prespawning), (2) 1 to 3 d post-major spawning, and (3) 4 to 5 d post-major spawning. The input of organic material 1 to 5 d post-major spawning also corresponded to the decrease in the net uptake of DON (Fig. 2; *see* Discussion below). A mixture of coral mucus with a C : N ratio of around 12 (Wild et al. 2005), turf algal detritus with a C : N ratio of around 8 (Hansen et al. 1992), and BMA detritus (Hansen et al. 1992) were the most likely sources of OM to the reef lagoon sediments before coral spawning. This is consistent with the prespawning sediment trap material C : N ratio of 10.5 and the low N deposition rates (Fig. 6; Wild et al. 2008). The high benthic flux remineralization ratios (>40) during these periods (Fig. 7) suggest that some of the mineralized N was not returned to the water column (*see* Eyre and Ferguson 2005 for discussion). The decreased remineralization ratios of around 32 as seen 1 to 3 d post-major spawning (Fig. 7), the increased N deposition rates, and the sediment trap material C : N ratio 14.4 to 17.2 most likely reflect the deposition and decomposition of large quantities of coral eggs and sperm, which had a molar C : N ratio of 20.3. Low benthic flux remineralization ratios of around 10, as seen on days 4 and 5 post-major spawning, are indicative of the benthic decomposition of N-rich OM such as phytoplankton detritus (Fig. 7). This coincides with elevated water column chlorophyll *a* concentrations (phytoplankton biomass) and a second smaller peak in phytoplankton and BMA production (Glud et al. 2008), a rapid increase in N deposition rates, and a decrease in the C : N ratio of material in the sediment trap. The larger peak in primary production 1 day post-major spawning probably resulted in little deposition of phytodetritus because of high grazing in the water column as reflected in the low water column biomass (Glud et al. 2008). Much of the N from the phytodetritus was denitrified via coupled nitrification–denitrification as shown by the high dark N_2 efflux and dark nitrate efflux on day 4 post-major spawning (Fig. 2). Remineralization ratios were slightly higher than expected for the likely sources of OM being decomposed (i.e., 10 > Redfield [6.6]; 32 > 16 to 21), also suggesting that some, albeit a smaller proportion, of the remineralized N was not returned to the water column. Alternatively, there may have been some mineralization in the water column before deposition in the sediments, or there was some high C : N

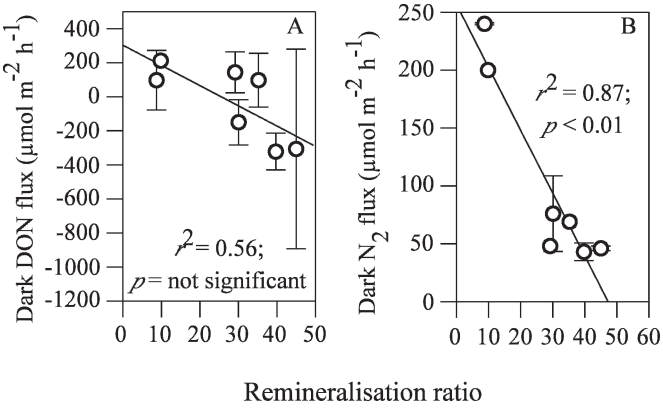

Fig. 8. (A) Remineralization ratio versus dark DON flux and (B) remineralization ratio versus dark N_2 flux.

material (e.g., BMA extracellular organic carbon [EOC]) being mineralized with the lower C : N material.

There was a weak negative relationship between dark DON fluxes and the C : N ratio of remineralized material ($r^2 = 0.56$; not significant, $p = 0.05$; Fig. 8A). The dark DON efflux at low remineralized C : N ratios is probably the hydrolysis product of fresh phytodetritus (Burdige and Zheng 1998; Eyre and Feguson 2005). Alternatively, the dark DON efflux at low (and mid-) remineralized C : N ratios occurred around maximum benthic productivity (Glud et al. 2008), suggesting that the DON may have been released via nighttime grazing of BMA (Eyre and Ferguson 2002). The dark DON uptakes at higher remineralized C : N ratios may be due to assimilation by heterotrophic bacteria. This demand would decrease when low C : N material is decomposed and when more water column N is available. Dark DON and NH_4^+ fluxes were negatively correlated post-major spawning ($r^2 = 0.55$; not significant, $p = 0.05$) with the increased dark uptake of NH_4^+ driven by higher concentrations in the water column, particularly at night when the incubation water was enclosed. Recent ^{15}N tracer experiments in the sediments of a subtropical estuary demonstrated that the microbial community uses both urea and amino acids (labile DON) as well as NO_3^- and NH_4^+ as N sources (Veuger et al. 2007). Other studies have shown that heterotrophic marine bacteria can assimilate urea (Jahns 1992), mangrove bacteria can assimilate dissolved free amino acids (Stanley et al. 1987), and DON is an energy source for benthic respiration, particularly by sulfate reducers (Guldberg et al. 2002). In tropical coral reef environments where there is very little freely available DIN, labile DON is probably the major N source for heterotrophic bacteria and the associated DOC may be an additional source of labile carbon for benthic metabolism (Eyre and Ferguson 2005). Benthic DON fluxes were generally an order of magnitude greater than DIN fluxes. The dark DON flux versus remineralized C : N ratio relationship is similar to the net DON flux versus remineralized C : N ratio relationship observed in the sediments of the subtropical Brunswick Estuary (Eyre and Ferguson 2005), but the slope is much steeper, with a large uptake of DON for a given remineralized C : N ratio.

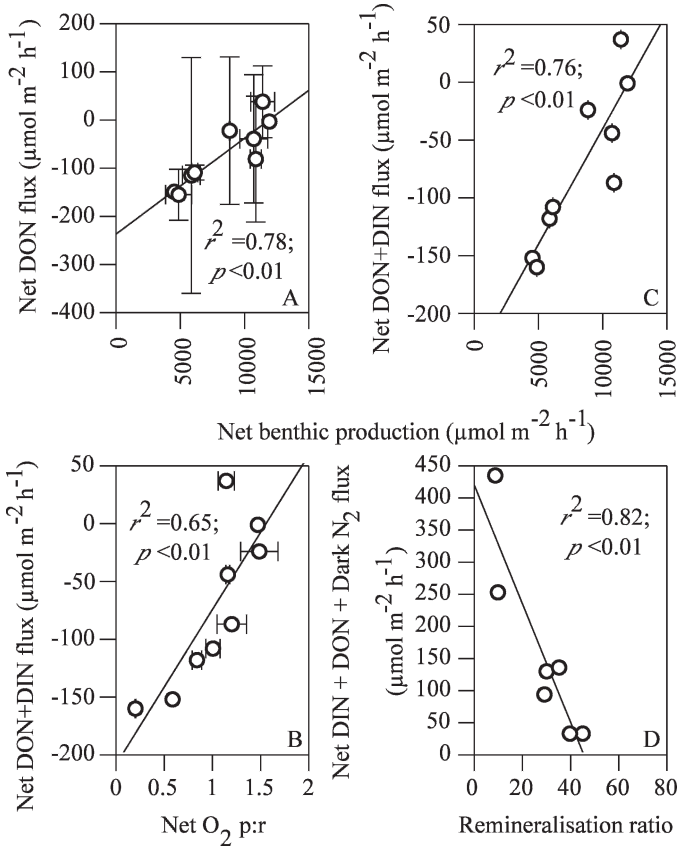

Fig. 9. Plots showing some of the major controls on benthic nitrogen fluxes: (A) net benthic production versus net DON flux, (B) net benthic production versus net DON + DIN flux, (C) net O_2 p : r versus net DON + DIN, and (D) remineralization ratio versus net DON + DIN + dark N_2 flux.

Water column DIN concentrations and dark benthic DIN fluxes in the coral reef lagoon were around an order of magnitude lower than in the subtropical Brunswick Estuary (Eyre and Ferguson 2005). The high demand for DON most likely reflects the combination of the high bacterial productivity and growth rates seen in coral reef benthos (Alongi 1994) and the low availability of DIN.

Before spawning, adsorption of water column P onto calcium carbonate in the sediments (e.g., coral fragments) probably contributed to the DIP uptake. With the exception of immediately (1 d) post-minor and post-major spawning, dark DIP uptakes over the study period were strongly negatively related to benthic respiration rates ($r^2 = 0.96$; $p < 0.01$). The increased decomposition of OM after coral spawning would have produced carbon dioxide and acids, which in turn may have dissolved some of the calcium carbonate, resulting in less adsorption of P. However, we have no pH data as evidence of these processes occurring. Immediately (1 d) post-minor and post-major spawning there was also a decrease in DIP uptake, but little increase in respiration rates (Glud et al. 2008), suggesting that the decreases in dark DIP uptake were probably due to more P available in the pore water from the decomposition of P-rich OM spawn material (162 $\pm$ 6 μmol g^{-1}) relative to the calcium carbonate adsorption

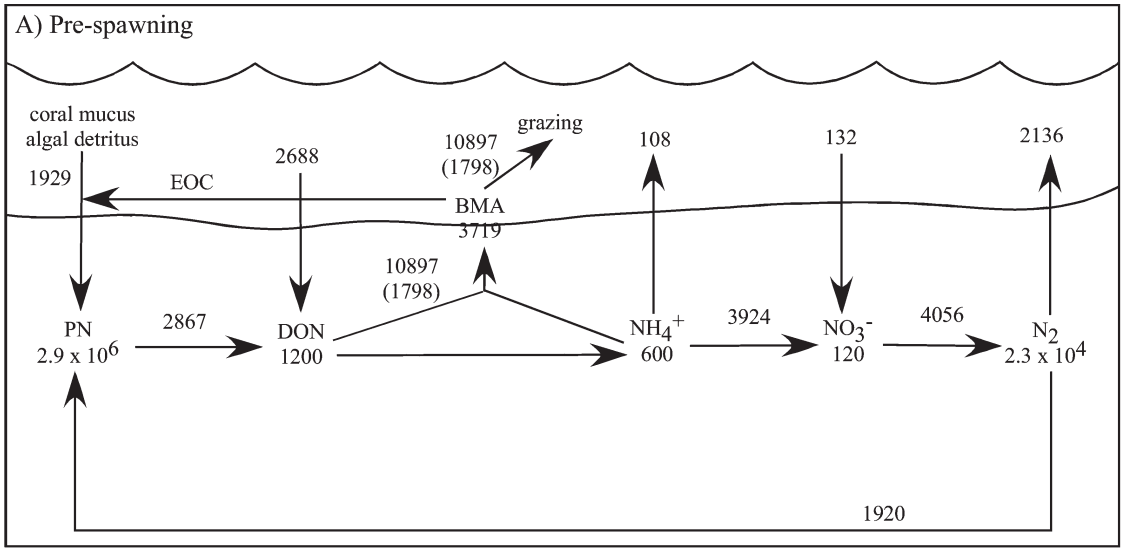
A) Pre-spawning
coral mucus
algal detritus
1929
EOC
2688
10897
(1798)
grazing
BMA
3719
108
132
2136
10897
(1798)
PN
2.9 x 10^6
2867
DON
1200
NH4+
600
3924
NO3-
120
4056
N2
2.3 x 10^4
1920

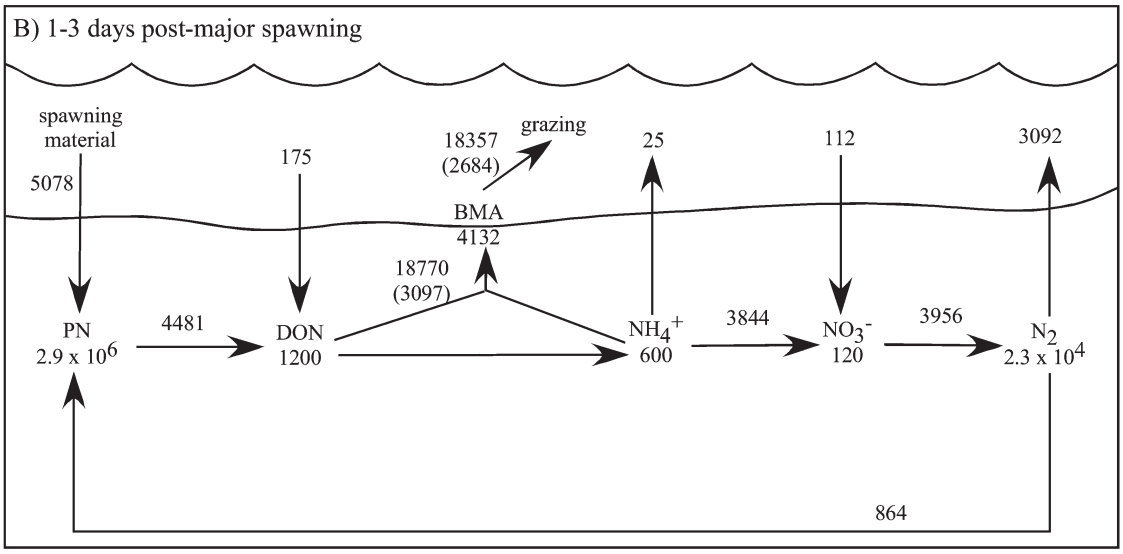
B) 1-3 days post-major spawning
spawning
material
5078
175
18357
(2684)
grazing
BMA
4132
25
112
3092
18770
(3097)
PN
2.9 x 10^6
4481
DON
1200
NH4+
600
3844
NO3-
120
3956
N2
2.3 x 10^4
864

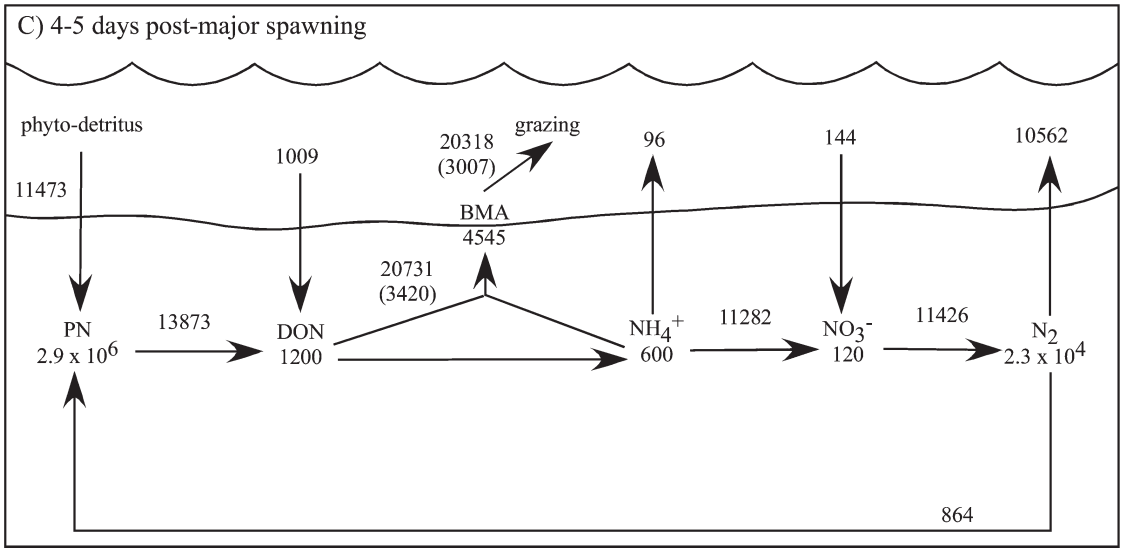
C) 4-5 days post-major spawning
phyto-detritus
11473
1009
20318
(3007)
grazing
BMA
4545
96
144
10562
20731
(3420)
PN
2.9 x 10^6
13873
DON
1200
NH4+
600
11282
NO3-
120
11426
N2
2.3 x 10^4
864

sites. Consistent with this was the increase in sediment bioavailable P and the efflux of DOP 1 d post-major spawning (the largest P efflux over the study period); mineralization of DOP would be a source of DIP. The slight effect of coral spawning on benthic P fluxes decreased by day 6 post-major spawning, but still had not returned to prespawning conditions by the end of the study period.

Benthic autotrophic metabolism and nutrient cycling—Benthic production exerted a strong influence on the benthic cycling of N over the study period, but little influence on the cycling of P. The largest N flux in the light was an uptake of DON, most likely due to assimilation by BMA. Several studies in temperate systems have demonstrated that BMA use the various components of DON as a N source (Admiraal et al. 1987; Nilsson and Sundback 1996; Linares 2005). Similar to phytoplankton and heterotrophic bacteria in tropical coral reef environments where there is very little freely available DIN (*see* above discussion), labile DON is probably also the major N source for BMA. For example, light and net NH_4^+ and NO_3^- fluxes were unrelated to net benthic production (both $r^2 < 0.01$; not significant; $p = 0.05$). However, BMA appeared to have quickly switched to other N sources when it became available post-major coral spawning as illustrated by the decrease in net DON uptake as benthic production increased ($r^2 = 0.78$; $p < 0.01$; Fig. 9A). Both the increase in benthic production and the decreasing importance of DON as a N source were probably driven by the higher availability of pore-water N (NH_4^+?) sourced from OM decomposition post-major spawning. The increase in pore-water N is illustrated immediately post-major spawning when there was a dark efflux of NH_4^+ (Fig. 2). This rapid increase in benthic production when more N became available reflects strong N limitation, which has also been shown for BMA in coral reef sediments (Dizon and Yap 1999; Heil et al. 2004; Clavier et al. 2005). However, despite these numerous previous studies of the interaction between BMA and N in coral reef sediments (e.g., Dizon and Yap 1999; Heil et al. 2004; Clavier et al. 2005), only one other study has considered DON as a N source (Boucher and Clavier 1990); Boucher and Clavier (1990) also found an uptake of DON by the benthos (bacteria and BMA) in sandy sediments.

Several previous studies of euphotic sediments in subtropical and warm temperate coastal systems have shown the sediment production : respiration (p : r) ratio to be a good predictor of net benthic N fluxes (e.g., Eyre and Ferguson 2002, 2005). N is generally assimilated as the sediment p : r increases (more autotrophic) and released as the sediment p : r decreases (more heterotrophic), with zero flux at the p : r that corresponds to maximum competition between the autotrophs, chemoautotrophs, and heterotrophs. In contrast, sediment p : r was not as good a predictor of the DON + DIN flux ($r^2 = 0.65$; $p < 0.01$; Fig. 9B) as net benthic productivity ($r^2 = 0.82$; $p < 0.01$; Figure 9C), and the relationship was the opposite of previous studies because the uptake and release of DON + DIN was mostly controlled by the availability of pore-water N. As more pore-water N became available from the decomposition of coral spawning material and associated phytodetritus, benthic productivity increased more rapidly than O_2 consumption (i.e., increasing p : r; Glud et al. 2008), but the demand by heterotrophs and autotrophs for water column DON decreased. The dark efflux of DON associated with either the grazing of BMA at high net productivities or the hydrolysis product of fresh phytodetritus also contributed to the decrease in net DON flux with increasing p : r. Sediment p : r has also been shown to be an important control on net N_2 fluxes (Eyre and Ferguson 2002, 2005), but unfortunately the data required for this assessment were not available because of bubble formation associated with the highly productive sediments. The best overall predictor of the total benthic N flux (net DIN + DON + dark N_2) was the remineralized C : N ratio ($r^2 = 0.79$; $p < 0.01$; Figure 9D), a proxy for the quality of OM. This relationship is driven by the control of pore-water N availability on both the uptake of water column DON and coupled nitrification–denitrification. When smaller amounts of low-quality OM were mineralized prespawning there was little net release of N from the sediments (Fig. 9D). N was tightly recycled and conserved prespawning, with any loss via N_2 offset by an uptake of DON. The large episodic input of medium-quality (C : N 15.9) OM post-major spawning results in a decrease in the uptake of DON due to a higher availability of pore-water NH_4^+ and a net loss of N, mostly as N_2, from the sediment (Fig. 9D). When high-quality, low-C : N (Redfield) phytodetritus was mineralized there was no uptake of DON and a large loss of N via denitrification (Fig. 9D).

Influence of the stirring gradient on benthic fluxes—Recent modeling has suggested that N_2 may be flushed out of the permeable sediments when advective flow rates are

←

Fig. 10. Benthic nitrogen budgets for the upper 10 cm of sediment in the Heron Island reef lagoon (A) prespawning, (B) 1 to 3 d post-major spawning, and (C) 4 to 5 d post-major spawning. Fluxes: μmol m^{-2} d^{-1} N; pools: μmol m^{-2} N. The bracketed value for the BMA uptake results in a balanced budget (*see* Discussion). All of the nitrogen flux rates were directly measured except ammonification and BMA assimilation. Nitrogen deposition rates are derived from Wild et al. (2008). Ammonification rates were calculated from benthic O_2 consumption rates (Glud et al. 2008) and the C : N ratio of the most likely depositing organic matter (*see* Discussion). BMA assimilation flux rates were calculated from the net benthic production rates and a C : N uptake ratio of 6.6 : 1. The sediment PN pool was also measured. The other sediment pools were calculated as follows: DON = 20 μmol L^{-1} (Burdige and Zeng 1998) × porosity × sediment volume (1×10^5 cm^3); NH_4^+ = 10 μmol L^{-1} (Williams et al. 1985; Capone et al. 1992) × porosity × sediment volume; NO_3^- = 2 μmol L^{-1} (Williams et al. 1985; Miyajima et al. 2001) × porosity × sediment volume; N_2 = solubility on the basis of temperature (25°C) and salinity (37); BMA = measured chlorophyll *a* (Chl *a*) (Glud et al. 2008) × 30 (Chl *a* : C) divided by 6.6 (C : N); grazing = nitrogen assimilation minus change in biomass.

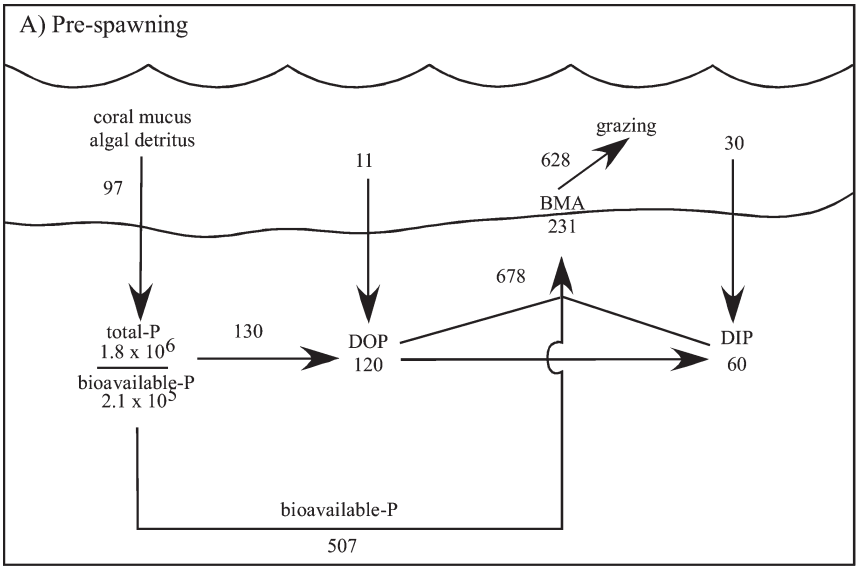
A) Pre-spawning
coral mucus
algal detritus
97
11
grazing
628
30
BMA
231
678
total-P
1.8 x 10^6
130
DOP
120
DIP
60
bioavailable-P
2.1 x 10^5
bioavailable-P
507

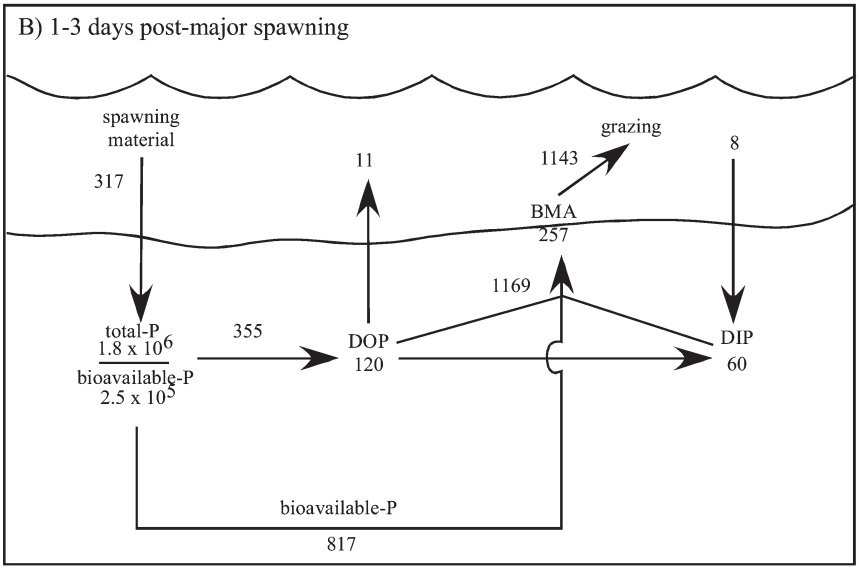
B) 1-3 days post-major spawning
spawning
material
317
11
grazing
1143
8
BMA
257
1169
total-P
1.8 x 10^6
355
DOP
120
DIP
60
bioavailable-P
2.5 x 10^5
bioavailable-P
817

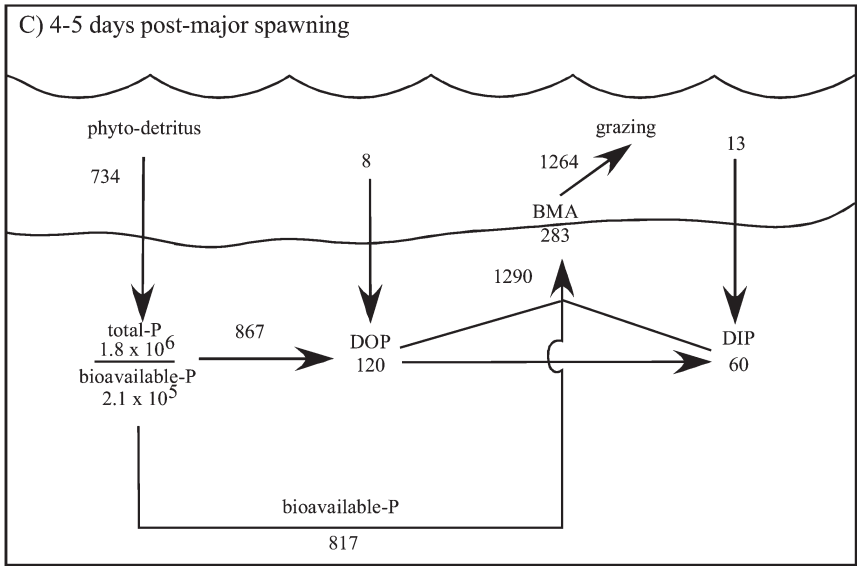
C) 4-5 days post-major spawning
phyto-detritus
734
8
grazing
1264
13
BMA
283
1290
total-P
1.8 x 10^6
867
DOP
120
DIP
60
bioavailable-P
2.1 x 10^5
bioavailable-P
817

increased (Cook et al. 2006). If there is a concentration gradient and percolation is induced a similar "washout" will occur with other solutes (i.e., NH_4^+, NO_3^-, DON, DIP) so the changes in flux rates with changing advective flow rates (Fig. 4) may be associated with either changes in biogeochemical processes or artifacts induced by nonsteady-state interstitial flow patterns and solute distribution. However, there is some evidence to suggest that some of the flux rate changes may be due to changes in biogeochemical processes. For example, the increasing uptake of DON and DIP in the light with increasing stirring rate (Figs. 2, 3) corresponds to an increase in benthic production (Glud et al. 2008), most likely due to assimilation of DON and DIP by BMA (as previously discussed). It is possible that the increase in N_2 effluxes with increasing advective flow was due to the increased downward transport of oxygen and enhanced coupled nitrification–denitrification, although modeling suggests that coupled nitrification–dentrification may decrease with increased flushing in sandy sediments because of the lack of anoxic denitrification sites (Cook et al. 2006). The large uptake of N_2 in the diffusive chambers on day 7 post-major spawning is difficult to explain and is most likely associated with a transient shift in interstitial solute distribution after a reduction in pore-water flow (Cook et al. 2006). Alternatively, the sediment microbial community may be starved of nitrogen with no advective flow and become net N fixing.

N and P budgets were constructed for the pre-, 1 to 3 d post-, and 4 to 5 d post-major spawning periods (Fig. 10). The most obvious outcome of the N budgets is that they do not balance with a larger uptake of N by BMA than can be explained by the inputs. This is most easily explained by nonsteady state induced by the chambers in the sandy sediments; steady state is an essential criterion for a balanced budget (Eyre and McKee 2002). However, there is some evidence to suggest that the system may have been close to steady state. For example, the measured rates of deposition of OM provided a reasonable balance to the estimated ammonification rates (Fig. 10). Alternatively, the N budget could be balanced if a C : N uptake ratio of 40 : 1 was applied to the net benthic production rates (*see* brackets in BMA assimilation term, Fig. 10). This may be reasonable as tropical BMA have a high production ratio of high C : N EOC because of high irradiance and low nutrient availability, particularly in coral sands (Underwood 2002), although such a high production of EOC is less likely for dinoflagellates that dominated the benthic bloom (Glud et al. 2008). Balanced or unbalanced, the N budgets are the most detailed constructed for coral reef sediments and as such, they provide several new insights into the benthic cycling of N in these systems.

During all three periods remineralized N and the N pools were rapidly recycled on a timescale of hours, with much of the N either lost via coupled nitrification–denitrification or assimilated by BMA (Fig. 10). Prespawning ammonification rates were also similar to the upper rates measured in other studies in coral reef sands and muds (Williams et al. 1985; Capone et al. 1992; Alongi et al. 2006), but the postspawning ammonification rates were much higher, reflecting the large episodic input of labile carbon (and N). The rapid response of BMA and denitrification to the increased supply of N post-major spawning illustrates that N was a limiting factor for both these pathways. Intense grazing of BMA by holothurians post-major spawning (pers. obs.) and rapid turnover (1 to 2 d) of the BMA N pool (Fig. 10) suggest that a large proportion of the assimilated N is removed via grazing. Previous studies in coral reef sands and muds have also highlighted the rapid turnover of N pools (Capone et al. 1992; Alongi et al. 2006) and the dominance of BMA assimilation (Miyajima et al. 2001). Rates of N assimilation by BMA were much higher than previous studies in coral reef sediments (Miyajima et al. 2001). Our work in particular has highlighted the importance of denitrification, which has previously probably been underestimated in coral reef sediments. Our work has also highlighted the importance of DON fluxes across the sediment–water interface, which were quantitatively very significant prespawning, and could account for 68% of the N needed for coupled nitrification–denitrification and over 100% of the N assimilated by BMA (balanced budget). Post-major spawning DON fluxes across the sediment–water interface were quantitatively a less significant component of the benthic N budget, but could still account for 29% of the N assimilated by BMA (balanced budget). DIN fluxes across the sediment–water interface were an insignificant component of benthic N cycle. N fixation was also quantitatively very significant prespawning, and could account for 49% of the N needed for coupled nitrification–denitrification and over 100% of the

←

Fig. 11. Benthic phosphorus budgets for the upper 10 cm of sediment in the Heron Island reef lagoon (A) prespawning, (B) 1 to 3 d post-major spawning, and (C) 4 to 5 d post-major spawning. Fluxes: μmol m^{-2} d^{-1} P; pools: μmol m^{-2} P. All of the phosphorus flux rates were directly measured except BMA assimilation. N : P ratios of 20, 16, and 16 for the prespawning, 1 to 3 d post-major spawning, and 4 to 5 d post-major spawning, respectively, were applied to nitrogen deposition rates (Wild et al. 2008) to estimate phosphorus deposition rates. A C : P ratio of 106 was applied to the benthic production rates to estimate BMA P assimilation rates. Bioavailable P flux equals the budget deficit ± error. The sediment PP pool was also measured. The other sediment pools were calculated as follows: DOP = 2.0 μmol L^{-1} (estimate) × porosity (0.55) × sediment volume (1×10^5 cm^3); DIP = 1.0 μmol L^{-1} (Suzumura et al. 2002) × porosity (0.55) × sediment volume; BMA = measured Chl *a* (Glud et al. 2008) × 30 (Chl *a* : C) divided by 106 (C : P); grazing = phosphorus assimilation minus change in biomass.

N assimilated by BMA (balanced budget). Similar to DON, N fixation became a quantitatively less significant component of the benthic N budget post-major spawning.

The most striking feature of the P budgets is the high demand by BMA that is not supported by uptakes of DIP or DOP across the sediment–water interface, pore-water P, or remineralized P (Fig. 11). Suzumura et al. (2002) also found that the P demand of BMA in coral reef sediments in Japan was up to two orders of magnitude greater than could be supplied by sediment–water fluxes of DIP (DOP was not measured) or pore-water P. In contrast, the P requirements of BMA in Tikehau Atoll were met by remineralized P (Charpy and Charpy-Roubaud 1988). In the absence of other P sources, benthic production was most likely supplied by the sediment pool of bioavailable P (Entsch et al. 1983; Suzumura et al. 2002). It is most likely this large pool of bioavailable P in the sediments that drives potential N limitation of benthic coral reef communities. The benthic community may ultimately be P limited on geological timescales because it can replenish N via N fixation, but on shorter timescales it is N limited because of the large pool of bioavailable P in the sediments. This was illustrated immediately post-major spawning with the P demand from increased benthic production, stimulated by N from the spawning material, met from the bioavailable P in the sediments (Fig. 5). There was sufficient bioavailable P stored in the top 10 cm of the sediment column to sustain the prespawning rates of benthic production for over 200 d. The sediment pool of P in turn must be replenished by the deposition of particulate organic (e.g., zooxanthellae, turf algae, mucus, phytodetritus, coral spawning material) and inorganic (e.g., coral fragments) P. However, because of the large pool of bioavailable P in the sediment, the input of P via the deposition of coral spawning material and associated phytodetritus results in only minor changes to P cycling in the sediments. This contrasts with sediment N cycling, which showed dramatic changes after coral spawning due to smaller bioavailable pools in the sediment and potentially N-limited benthic communities.

References

Admiraal, W., C. Riaux-Gobin, and R. W. P. M. Laane. 1987. Interactions of ammonium, nitrate and D- and L-amino acids in the nitrogen assimilation of two species of estuarine benthic diatoms. Mar. Ecol. Prog. Ser. **40:** 267–273.

Alongi, D. M. 1994. The role of bacteria in nutrient cycling in tropical mangrove and other coastal benthic ecosystems. Hydrobiology **285:** 19–32.

———, J. Pfitzner, and L. A. Trott. 2006. Deposition and cycling of carbon and nitrogen in carbonate mud of the lagoons of Arlington and Sudbury Reefs, Great Barrier Reef. Coral Reefs **25:** 123–143.

Arai, T., M. Kato, A. Heyward, Y. Ikeda, T. Lizuka, and T. Maruyama. 1993. Lipid composition of positively buoyant eggs of reef building corals. Coral Reefs **12:** 71–75.

Baird, A. H., M. S. Pratchett, D. J. Gibson, N. Koziumi, and C. P. Marquis. 2001. Variable palatability of coral eggs to a planktivorous fish. Mar. Freshwat. Res. **52:** 865–868.

Birch, G., B. D. Eyre, and S. E. Taylor. 1999. The distribution of nutrients in the bottom sediments of Port Jackson (Sydney Harbour), Australia. Marine Pollution Bulletin **38:** 1247–1251.

Boucher, G., and J. Clavier. 1990. Contribution of benthic biomass to overall metabolism in new Caledonia lagoon sediments. Mar. Ecol. Prog. Ser. **64:** 271–280.

Burdige, D. J., and S. Zheng. 1998. The biogeochemical cycling of dissolved organic nitrogen in estuarine sediments. Limnol. Oceanogr. **43:** 1796–1813.

Capone, D. G. 1993. Determination of nitrogenase activity in aquatic samples using acetylene reduction procedure, p. 621–632. *In* P. F. Kemp, B. F. Sherr, E. B. Sherr and J. J. Cole [eds.], Aquatic microbial ecology. Lewis.

———, S. E. Dunham, S. G. Horrigan, and L. E. Duguay. 1992. Microbial nitrogen transformations in unconsolidated coral reef sediments. Mar. Ecol. Prog. Ser. **80:** 75–88.

Charpy, L. 2001. Phosphorus supply for atoll biological productivity. Coral Reefs **20:** 357–360.

———, and C. J. Charpy-Roubaud. 1988. Phosphorus budget in an atoll lagoon. Proc. Sixth Int. Coral Reef Symp. **2:** 547–550.

Clavier, J., G. Boucher, L. Chauvaud, R. Fichez, and S. Chifflet. 2005. Benthic response to ammonium pulses in a tropical lagoon: Implications for coastal environmental processes. J. Exp. Mar. Biol. Ecol. **316:** 231–241.

Cook, P. M., and others. 2006. Quantification of denitrification in permeable sediments: Insights from a two dimensional simulation and experimental data. Limnol. Oceanogr. Methods **4:** 294–307.

Delesalle, B., M. Pichon, M. Frankignoulle, and J. P. Gattuso. 1993. Effects of a cyclone on coral reef phytoplankton biomass, primary production and composition (Moorean Island, French Polynesia). J. Plankton Res. **15:** 1413–1423.

Dizon, R. M., and H. T. Yap. 1999. Short-term responses of coral reef microphytobenthic communities to inorganic nutrient loading. Limnol. Oceanogr. **44:** 1259–1267.

Entsch, B., K. G. Boto, R. G. Sim, and J. T. Wellington. 1983. Phosphorus and nitrogen in coral reef sediments. Limnol. Oceanogr. **28:** 465–476.

Erftemeijer, P. L. A., and J. J. Middelburg. 1993. Sediment–nutrient interactions in tropical seagrass beds: A comparison between a terrigenous and a carbonate sedimentary environment in South Sulawesi (Indonesia). Mar. Ecol. Prog. Ser. **102:** 187–198.

Eyre, B. D. 1993. Nutrients in the sediments of a tropical north-eastern Australian estuary, catchment and nearshore coastal zone. Aust. J. Mar. Freshwat. Res. **44:** 845–866.

———. 2000. A regional evaluation of nutrient transformation and phytoplankton growth in nine river dominated sub-tropical East Australian estuaries. Mar. Ecol. Prog. Ser. **205:** 61–83.

———, and A. J. P. Ferguson. 2002. Comparison of carbon production and decomposition, benthic nutrient fluxes and denitrification in seagrass, phytoplankton, benthic microalgal and macroalgal dominated warm temperate Australian lagoons. Mar. Ecol. Prog. Ser. **229:** 43–59.

———, and ———. 2005. Benthic metabolism and nitrogen cycling in a sub tropical east Australian estuary (Brunswick): Temporal variability and controlling factors. Limnol. Oceanogr. **50:** 81–96.

———, and ———. 2006. Impact of a flood event on benthic and pelagic coupling in a sub-tropical east Australian estuary (Brunswick). Estuar. Coast. Shelf Sci. **66:** 111–122.

———, AND L. MCKEE. 2002. Carbon, nitrogen and phosphorus budgets for a shallow sub-tropical coastal embayment (Moreton Bay, Australia). Limnol. Oceanogr. **47:** 1043–1055.

———, S. RYSGAARD, T. DALSGAARD, AND P. B. CHRISTENSEN. 2002. Comparison of isotope pairing and N2/Ar methods for measuring sediment denitrification rates—assumptions, modifications and implications. Estuaries **25:** 1077–1087.

FURNAS, M. J., A. W. MITCHELL, M. GILMARTIN, AND N. REVELANTE. 1990. Phytoplankton biomass and primary production in semi-enclosed reef lagoons of the central Great Barrier Reef, Australia. Coral Reefs **9:** 1–10.

———, A. MITCHELL, M. SKUZA, AND J. BRODIE. 2005. In the other 90%: Phytoplankton responses to enhanced nutrient availability in the Great Barrier Reef Lagoon. Mar. Pollut. Bull. **51:** 253–265.

GLUD, R. N., B. D. EYRE, AND N. PATTERN. 2008. Biogeochemical responses to mass coral spawning on the Great Barrier Reef: Effects on respiration and primary production. Limnol. Oceanogr **53:** 1014–1024.

GULDBERG, L. B., K. FINSTER, N. O. G. JORGENSEN, M. MIDDELBOE, AND B. A. LOMSTEIN. 2002. Utilization of marine sedimentary dissolved organic nitrogen by native anaerobic bacteria. Limnol. Oceanogr. **47:** 1712–1722.

HAGMAN, D., S. GITTINGS, AND K. DESLARZES. 1998. Timing, species participation and environmental factors influencing annual mass spawning at the Flower garden banks (Northwest Gulf of Mexico). Gulf Mex. Sci. **16:** 170–179.

HANSEN, J. A., D. W. KLUMPP, D. M. ALONGI, P. K. DAYTON, AND M. J. RIDDLE. 1992. Detrital pathways in a coral reef lagoon. Mar. Biol. **113:** 363–372.

HARRISON, P. L., R. C. BABCOCK, G. D. BULL, J. K. OLIVER, C. C. WALLACE, AND B. L. WILLIS. 1984. Mass spawning in tropical reef corals. Science **223:** 1186–1189.

———, AND C. C. WALLACE. 1990. Reproduction, dispersal and recruitment of scleractinian corals, p. 133–207. *In* Z. Dubinsky [ed.], Coral reef ecosystems, V. 25. Elsevier Science Publishers.

HAYASHIBARA, T., AND OTHERS. 1993. Patterns of coral spawning at Akajima Island, Okinawa, Japan. Mar. Ecol. Prog. Ser. **101:** 253–262.

HEIL, C. A., K. CHASTON, A. JONES, P. BIRD, B. LONGSTAFF, S. COSTANZO, AND W. C. DENNISON. 2004. Benthic microalgae in coral reef sediments of the southern Great Barrier Reef, Australia. Coral Reefs **23:** 336–343.

HUETTEL, M., AND G. GUST. 1992. Solute release mechanisms from confined sediment cores in stirred benthic chambers and flume flows. Mar. Ecol. Prog. Ser. **82:** 187–195.

JAHNS, T. 1992. Urea uptake by the marine bacterium *Deleya venusta* HG1. J. Gen. Microbiol. **138:** 1815–1820.

KOOP, K., AND OTHERS. 2001. ENCORE: The effect of nutrient enrichment on coral reefs. Synthesis of results and conclusions. Mar. Pollut. Bull. **42:** 9–120.

LINARES, F. 2005. Effect of dissolved free amino acids (DFAA) on the biomass and production of microphytobenthic communities. J. Exp. Mar. Biol. Ecol. **330:** 469–481.

MIYAJIMA, T., S. MASAHIRO, Y. UMEZAWA, AND I. KOIKE. 2001. Microbial nitrogen transformation in carbonate sediments of a coral-reef lagoon and associated seagrass beds. Mar. Ecol. Prog. Ser. **217:** 273–286.

NILSSON, C., AND K. SUNDBACK. 1996. Amino acid uptake by natural benthic microalgal assemblages studied by microautoradiography. Hydrobiology **332:** 119–129.

PRATCHETT, M. S., N. GUST, G. GOBY, AND S. O. KLANTEN. 2001. Consumption of coral propagules represents a significant trophic link between corals and reef fish. Coral Reefs **20:** 13–17.

ROELFSEMA, C. M., S. R. PHINN, AND W. C. DENNISON. 2002. Spatial distribution of benthic microalgae on coral reefs determined by remote sensing. Coral Reefs **21:** 264–274.

RYSGAARD, S., R. N. GLUD, N. RYSGAARD-PETERSEN, AND T. DALSGAARD. 2004. Denitrification and anammox activity in Arctic sediments. Limnol. Oceanogr. **49:** 1471–1481.

RYSGAARD-PETERSEN, N., AND S. RYSGAARD. 1995. Nitrate reduction in sediments and waterlogged soil measured by ^{15}N techniques, p. 287–310. *In* K. Alef and P. Nannipieri [eds.], Methods in applied soil microbiology and biochemistry. Academic Press.

SIMPSON, C. J., L. J. CARY, AND R. J. MASINI. 1993. Destruction of corals and other reef animals by coral spawn slicks on Ningaloo reef, Western Australia. Coral Reefs **12:** 185–191.

STANLEY, S. O., K. G. BOTO, D. M. ALONGI, AND F. T. GILLAN. 1987. Composition and bacterial utilisation of free amino acids in tropical mangrove sediments. Mar. Chem. **22:** 13–21.

SUZUMURA, M., T. MIYAJIMA, H. HATA, Y. UMEZAWA, H. KAYANNE, AND I. KOIKE. 2002. Cycling of phosphorus maintains the production of microphytobenthic communities in carbonate sediments of a coral reef. Limnol. Oceanogr. **47:** 771–781.

THAMDRUP, B., AND T. DALSGAARD. 2002. Production of N_2 through anaerobic ammonium oxidation coupled to nitrate reduction in marine sediments. Appl. Environ. Microbiol. **68:** 1312–1318.

UNDERWOOD, G. J. C. 2002. Adaptations of tropical marine microphytobenthic assemblages along a gradient of light and nutrient availability in Suva Lagoon, Fiji. Eur. J. Phycol. **37:** 449–462.

VEUGER, B., B. D. EYRE, D. MAHER, AND J. J. MIDDELBURG. 2007. Nitrogen incorporation and retention by bacteria, algae, and fauna in a sub-tropical, intertidal sediment: An in-situ ^{15}N-labeling approach. Limnol. Oceanogr. **52:** 1930–1942.

WESTNEAT, M., AND J. RESING. 1988. Predation on coral spawn by planktivorous fish. Coral Reefs **7:** 89–92.

WILD, C., C. JANSEN, U. STRUCK, O. HOEGH-GULDBERG, AND M. HUETTEL. 2008. Biogeochemical responses following coral mass spawning on the Great Barrier Reef: Pelagic–benthic coupling. Coral Reefs **27:** 123–132.

———, R. TOLLRIAN, AND M. HUETTEL. 2004. Rapid recycling of coral mass-spawning products in permeable reef sediments. Mar. Ecol. Prog. Ser. **271:** 159–166.

———, H. WOYT, AND M. HUETTEL. 2005. Influence of coral mucus on nutrient fluxes in carbonate sands. Mar. Ecol. Prog. Ser. **287:** 87–98.

WILLIAMS, S. L., I. P. GILL, AND S. M. YARISH. 1985. Nitrogen cycling in backreef sediments, p. 389–394. *In* Proceedings of the 5th International Coral Reef Congress, Tahiti.

WOLANSKI, E., D. BURRAGE, AND B. KING. 1989. Trapping and dispersion of coral eggs around Bowden Reef, Great Barrier Reef, following mass coral spawning. Cont. Shelf. Res. **9:** 479–496.

Received: 15 May 2007
Accepted: 18 September 2007
Amended: 23 January 2008